Geometry and topology of Polish Outer Carpathian digital elevation model interpreted lineament network in context of regional tectonics

Maciej Kania[1], Mateusz Szczęch[1]

[1]Jagiellonian University in Kraków, Faculty of Geography and Geology, Institute of Geological Sciences, Gronostajowa 3a, 30-863 Kraków, Poland

Correspondence to: Maciej Kania (maciej.kania@uj.edu.pl)

Abstract. The Polish part of the Western Outer Carpathians lineament network was analysed based on the GMTED2010 digital elevation model. Lineaments were identified in the visual screening of the hillshade model. To the best of our knowledge, no one has studied the geometrical properties of the network with relation to the topological ones. The NetworkGT QGIS toolbox was applied to identify the nodes and branches of the network, as well as to calculate the topology parameters. Our aim was to find differences between the western and eastern parts of the Western Outer Carpathians; therefore, the analyses were carried out in six sectors chosen based on the geographical subdivision in the geological context: three in the north, mainly the Silesian unit; and three in the south, mainly the Magura unit. We found general agreement of the identified network with the photolineament map; however, some of the photolineaments are not confirmed by digital elevation model (DEM). We found that the topological parameters of the networks change from west to east, but not from north to south. There are areas of increased interconnectivity, especially the Nowy Sącz Basin, where the lineament network may reflect a complicated system of cross-cutting deep-rooted fault zones in the basement.

1. Introduction

Remote sensing imagery is an important source of data in regional tectonics, and its importance has been growing in recent years. Since the 1970s, there have been multispectral satellite photos of the Earth surface applied mainly in mineral mapping (e.g. van der Meer et al., 2012), as well as in tectonic studies (e.g. Leech et al., 2003). The Shuttle Radar Topography Mission (SRTM) resulted in the first remote sensing digital elevation model of most of the continental surface of the planet, with immense potential for application in geology (Yang et al., 2011). Then, new superior resolution and quality models were created on both the global (satellite) and local scale (mainly airborne LiDAR scanning). Digital elevation models are especially useful in areas with lush vegetation. The application of LiDAR in the Carpathians' flysch-type mountains in geological interpretations was shown, for example, in Kania and Szczęch (2022).

Our previous study (Kania and Szczęch, 2020), based on the interpretation of the model augmented with field geological mapping (Szczęch and Cieszkowski, 2021), showed how a lineament network can be interpreted in topological and geometrical terms. The aim in the present paper is to up-scale DEM-based geometrical and topological analyses of a regional scale lineament network to find how this is reflected in the tectonic structure of the Western Carpathians. Previous studies of the Carpathian lineaments were mainly focused on lineament strikes distribution (e.g. Doktór and Graniczny, 1982, 1983; Doktór et al., 1985, 1990, 2002; Bażyński et al., 1986; Graniczny and Mizerski, 2003)**;** therefore, we decided to add an interconnectivity aspect in terms of the topological parameters (Valentini et al., 2007; Sanderson and Nixon, 2015; Thiele et al., 2016), as a way of better understanding the structural problems. Most of the Carpathian-related studies are geographically organised in mountain arc parallel belts, reflecting the main tectonostratigraphic units, now forming nappes and being sedimentary basins during the Carpathian flysch depositions. We decided to keep this subdivision, although combining this with physiographical subdivisions into sectors with borders perpendicular to the Carpathian belt.

2. Up-to-date research on the Polish Outer Carpathian lineaments

The fact that dislocation lines perpendicular to the Carpathian arc are related to the deep basement, and are significantly older than the Carpathians themselves, was postulated even before the remote sensing era (Teisseyre, 1907). The first modern attempts to interpret lineaments in the Polish Carpathians were based on the Landsat MSS imagery and Heat Capacity Mapping Mission satellite, and reported together with data from the whole territory of

48   Poland on a photogeological map at 1:1 000 000 scale (Graniczny and Mizerski, 2003; Bażyński et al., 1986). The
49   main lineament systems of the Western Carpathians in the context of structural geology were shown by Doktór
50   and Graniczny (1983) and Doktór et al. (1985). The results of satellite imagery lineament detections were then
51   correlated with geophysical data proving relationships between the surface, neotectonic processes and deep
52   Carpathian basement structure (Doktór et al., 1990; Motyl-Rakowska and Ślączka, 1984). Airborne radar data
53   were applied in tectonic analysis of the Carpathians, resulting in 17 000 short lineaments that were the basis of the
54   lineament density map (Doktór et al., 2002). The interpretation of SRTM hillshading visualisation was performed
55   by Chodyń (2004) on the limited area in Beskid Wyspowy Mts. Comparison of Landsat MSS and SRTM data by
56   Ozimkowski (2008) showed that whilst the main faults can be related to lineaments, there are still numerous
57   lineaments without geological explanation.

58   **3.   Study area**

59   The choice of the study area was based on the physiogeographical subdivision of Poland by Solon et al. (2018).
60   The following macroregions were selected: the Western Beskidy Foothills, Western Beskidy Mts., Orawa–Podhale
61   Basin, Mid-Beskidy Foothills and Mid-Beskidy Mts. These five regions, with a total area of 17 437 km², cover
62   most of the Polish part of the Outer Carpathians, excluding a small part of the Eastern Outer Carpathians located
63   in Poland.

64
65

66   **3.1   Geological setting of the study area**

67   The research area is located in the Polish sector of the Western Outer Carpathians (Mahel', 1974; Książkiewicz,
68   1977; Ślączka et al., 2006; Fig. 1). It contacts tectonically with the Pieniny Klippen Belt from the south, which is
69   a border between the Outer and the Central Carpathians (Plašienka, 2018; Golonka et al., 2019a, 2020, 2019b;
70   Książkiewicz, 1977). The Outer Carpathians are built mainly of flysch deposits, whose thickness is approximately
71   6 000 m, and thus they are also referred to as the Flysch Carpathians (Golonka et al., 2020; Ślączka et al., 2006;
72   Golonka et al., 2005; Książkiewicz, 1977). These deposits are Late Jurassic–Early Miocene in age and are mainly
73   deep-sea sediments deposited by the gravity flow in the several sedimentary basins of the Northern Tethetis,
74   separated by ridges (Golonka et al., 2005, 2020; Ślączka et al., 2006; Książkiewicz, 1977). The thrust of the Central
75   Carpathians block to the north on the European Platform blocks — the Brunovistulicum and Małopolska Massif
76   (Żaba, 1999) — led to the forming of the synorogenic stage accretionary prism. The sediments deposited in the
77   basins were folded and thrusted one upon another, creating the sequence of the nappes in the Miocene. Going from
78   the south there are the Magura Nappe, Dukla Nappe, Fore–Magura group of nappes, Silesian Nappe, Sub-Silesian
79   Nappe and Skole Nappe (Mahel', 1974; Książkiewicz, 1977; Golonka et al., 2005, 2019a; Ślączka et al., 2006).
80   The deposits of the Outer Carpathians are overthrust on the Miocene molasses filling the Carpathian Foredeep,
81   which was deposited on the front of the Outer Carpathian orogenic belt thrusting over the North European Platform
82   (Ślączka et al., 2006; Oszczypko, 2006).
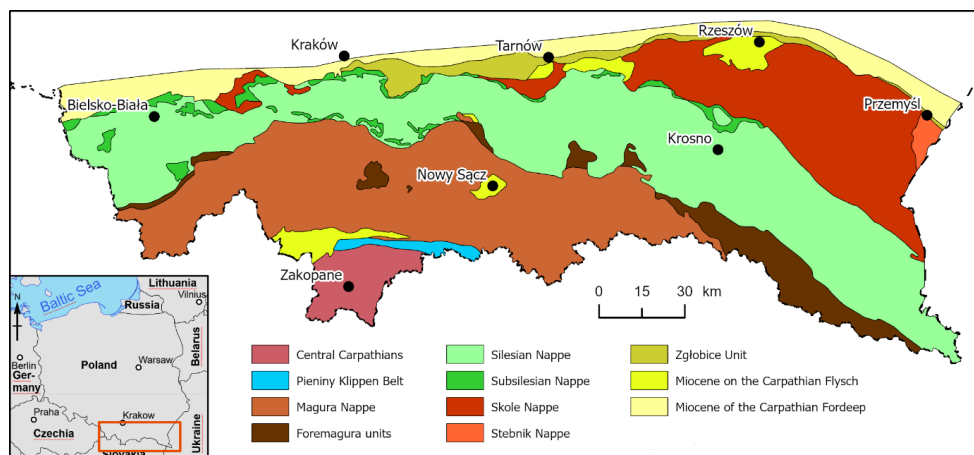
Fig. 1. Generalised geological map of the Polish part of the Carpathians based on Cieszkowski et al., 2017 and cited there.

3.2 Analysis of the sectors

We used the morphometry subdivision of Poland (Solon et al., 2018) to define the area, based on the subprovinces of the Western Outer Carpathians in the area of Poland and a small band of Northern Subcarpathia subprovince to the border of the Carpathians in the geological meaning (Carpathian overthrust on the Foredeep sediments), according to Lexa et al. (2000). The subdivision of the outer Carpathian belt is mostly used in the geology basis on the tectonostratigraphic units (nappes). This subdivision, however, does not allow differences in lineament systems parallel to the belt to be caught. The newly proposed morphostructural subdivision of the Western Carpathians (Minár et al., 2011) is another approach that compiles geological and morphological features. The Polish part of the Western Carpathians is subdivided into the following subregions (number according to the paper cited): (3f) Moravian–Silesian Beskid, (3a) Beskid Żywiecki–Gorce, (3b) Beskid Sądecki–Levočské vrchy, (5a) Beskid Wyspowy, (5b) Low Beskid and (6) North Foreland. The last subregion spans all the length of the northern Carpathian boundary between the Orava and San rivers. We decided to compile the geological subdivision with the morphological one (Solon et al., 2018), which also comprises a subdivision of the outermost units, into five sectors (Fig. 2, Tab. 1). The only change was including Ciecień Mount in Beskid Wyspowy into the Central Silesian sectors, as this massif, unlike all other Beskid Wyspowy culminations is built of Silesian series deposits.

102
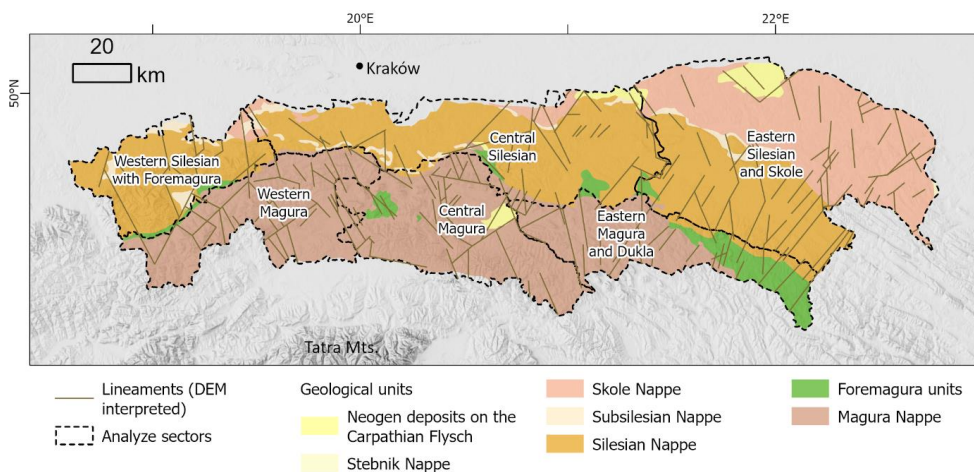
Fig. 2. Sectors defined based on the physiogeographical (Solon et al., 2018) and tectonic subdivisions
104 **(Golonka et al., 2020) of the study area (Western Outer Carpathians in Poland).**

105

106 **Tab. 1. Analyse sectors**

Analyse sectors name;	Symbol	Mesoregions covered according to Solon et al., 2018
Western Silesian with Foremagura	WS	Silesian Beskid Mts., Żywiec Basin, Silesia Foothils, Mały Beskid Mts.
Central Silesian	CS	Wieliczka Foothils, Wiśnicz Foothils, Beskid Wyspowy Mts – only the Ciecień ridge, Rożnów Foothils, Ciężkowice Foothils, Gorlice Basin
Eastern Silesian and Skole	ES	Przemyśl Foothils, Jasło-Krosno Basin, Strzyżów Foothills, Dynów Foothils, Jasło Foothils, Bukowiec Foothills
Western Magura	WM	Orawa-Jordanów Foothills, Orawa Interfluve, Koniaków Intermontane Region, Żywiec-Kysuce Beski, Pewel-Krzeczów Ranges, Makowski Beskid, Żywiec-Orawa Beskid
Central Magura	CM	Sącz Beskid Mts., Sącz Basin, Wyspowy Beskid (without Ciecień Ridge), Gorce Mts.
Eastern Magura and Dukla	EM	Low Beskid Mts.

107

108 **4.   Data and methods**

109 **4.1   Digital elevation model**

110 The Global Multi-resolution Terrain Elevation Data 2010 (GMTED2010; see Danielson, 2011) 7.5 arc-second

111 product was chosen as a work base. The model is a compilation of different raster-based elevation sources, based

112   mainly on SRTM digital terrain elevation data. The resolution is ca. 0.0021°/pixel, which means ca. 233 m/pixel.

113   This was found to be sufficient, while the working scale during lineament detection was 1:150 000. As the shading

114   azimuth can influence the results, the working imagery was multidirectional hillshade (Introducing Esri's Next

115   Generation Hillshade, 2022).

4.2   Multiple cover lineament detection

117   The manual method of lineament extraction was applied for two reasons. First, it is the simplest, low cost and

118   widely used method. The second reason is that it creates a basis for further work, based on automated extraction.

119   However, the method used is prone to some operator-related bias (Scheiber et al., 2015; Ehlen, 2004). Thus, to

120   reduce this bias the lineaments were extracted by two operators working independently, in three sessions, separated

121   by intervals of several months. After each session, the results were analysed and a network of common features

122   was created. The last stage was creating a concise network of lineaments based on the results of the three sessions.

123

4.3   Network analysis

125   A network can be described by scale-independent topological characteristics, based on the case of a line network

126   on graph theory. The network (graph) is formed by nodes (end or intersection points) connected by lines

127   (Sanderson and Nixon, 2015; Mukherjee, 2019). The line can be formed by one or more branches connected by

128   nodes. The node can be isolated (I type), an embranchment (Y type) or an intersection (X type), where the latter

129   two types are connecting nodes. Thus, the branch can connect two I type nodes (I–I branch), isolated and

130   connecting nodes (I–C branch, which can be I–Y or I–X) and two connecting nodes (C–C branch, which can be

131   X–X, X–Y or Y–Y). The proportion of nodes and branch types can be analysed as tertiary systems that characterise

132   the properties of the network, especially its interconnectivity (Procter and Sanderson, 2018; Sanderson and Nixon,

133   2015; Sanderson et al., 2018).

134   The spatial variation of the topological parameters of the network was analysed with the following aspects: (1)

135   regular, in a 5x5 km grid; and (2) within sectors based on the mesoregions of physiogeographical subdivision,

136   according to Solon et al. (2018) and the main tectonic units (Fig. 2 Tab. 1).

137   The NetworkGT QGis toolbox (Nyberg et al., 2018) was used as a tool in the topological analyses. The lineament

138   network was checked and repaired with NetworkGT tools. An additional stage was the manual correction of some

139   features to eliminate all non-defined types of nodes, as well as some extremely short (ca. 500 m or shorter) features.

140   The topological parameters were analysed in three modes: the whole network; the sectors defined; and in a regular,

141   5x5 km grid with 10 km search radius.

142   The Rayleigh test of semicircular distribution test was performed with the EZ-ROSE spreadsheet (Baas, 2000),

143   and circular statistics were calculated with the SciPy stats module (The SciPy Community, 2022).

5.   Results

5.1   Network geometry

146   The azimuths of the lineaments in all the analysed sectors show a multimodal distribution. Thus, the directions

147   were separated into sets, in a way that gives low values of circular variance. The angular ranges of all the sets are

148   presented in Tab. 2. For all sets, except for set 2 in the Eastern Magura (EM) sector and set 2 in the Western

149   Silesian (WS) sector, the distribution is not uniform, as checked with the Rayleigh test (Baas, 2000). The two sets

150   not checked were not numerous enough to be representative.
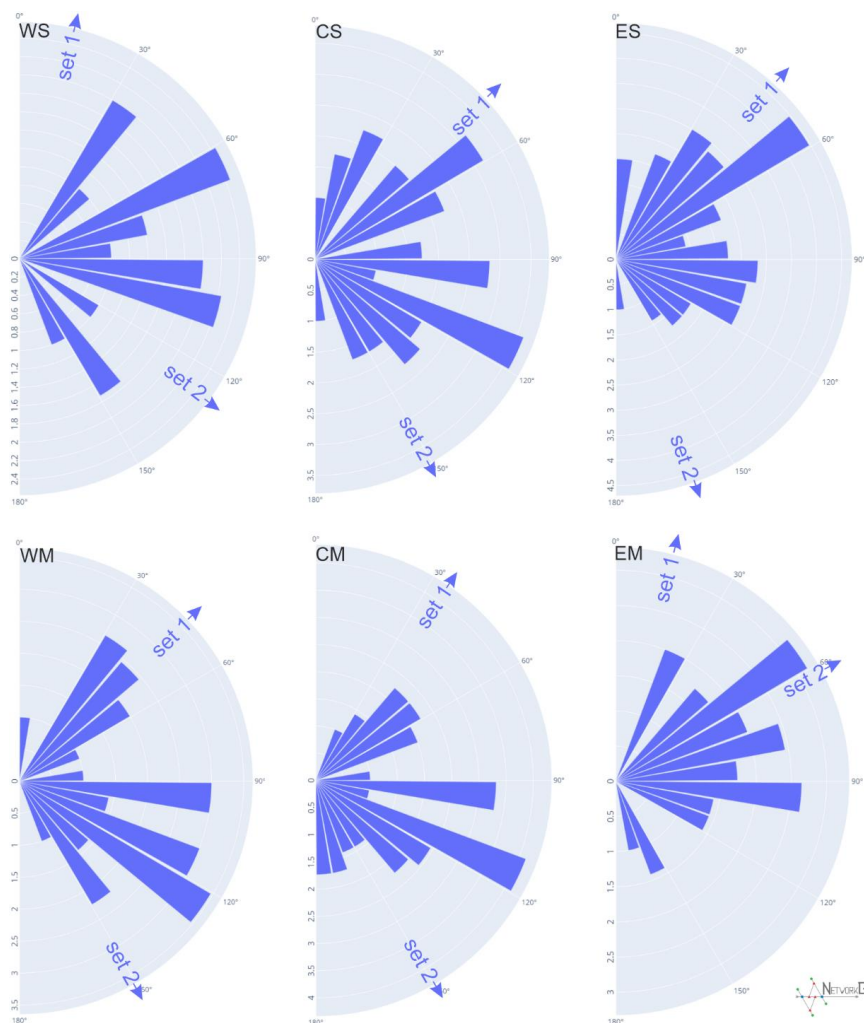
151

152   **Fig. 3: Rose diagrams of the analysed networks in the analytic sectors; upper row: Western Silesia with**

153   **Foremagura (WS), Central Silesia (CS), Eastern Silesia (ES); lower row: Western Magura (WM), Central**

154   **Magura (CM), and Eastern Magura (EM). Arrows mark the mean azimuth for the sets defined in Tab. 2.**

155

156   **Tab. 2. Azimuths of the lineaments in the analyse sectors**

Analyse sector	Set	Azimuths range	n	Circular statistics			The acute angle between sets means
				Mean	**Std. dev**	**Variance**	
CS	1	0 – 100	15	46.5	14.2	3.5	75.5
	2	100 – 180	13	151	16.6	4.8	

CM	1	0 – 80	17	34.1	13	3	63.9
	2	80 – 180	51	150.2	21.5	8.1	
EM	1	45 – 75	41	62.1	7.5	1.0	47.7
	2	0 – 45 75 – 180	3	14.4	26.7	12.5	
ES	1	0 – 100	59	42.7	19.7	6.8	62.1
	2	100 – 180	28	160.6	14.7	3.8	
WM	1	0 – 100	20	46.5	14.2	3.5	75.5
	2	100 – 180	40	151	16.6	4.8	
WS	1	0 – 60 150 – 180	23	13.6	23.3	9.5	66.2
	2	60 – 150	5	127.4	8.9	1.4	

157

158 The orientation of lineaments in all sectors, as well as the circular mean azimuth are shown in Fig. 3. In sectors

159 Central and Eastern Silesian (CS, ES) and Central and Western Magura (CM, WM) the set 1 mean is located

160 between 34° and 47°, marking a dominant SW–NE strike of lineaments. In the Western Silesian sector (WS), set

161 1 is oriented more to the north (14°). In all sectors above, there is a second set with a NW–SE trend, mostly oriented

162 at 150–160°, but in the Western Silesian sector case the mean azimuth is lower (127°), as in the case of the first

163 set. The last sector, Eastern Magura and Dukla, is different. There is one dominant set with azimuth 62°, and the

164 second set is poorly represented and oriented northward. The angle between the two sets varies in the 62–76°

165 range, except in the Eastern Magura and Dukla sector where it is only 48°.

166 **5.2   Network topology**

167 In the study area, 305 lineaments were marked in total. These features comprise 432 nodes. Of this count, 58% are

168 I nodes, 19% are E nodes, 18% are Y nodes and 5% are X nodes. The network contains 338 branches, within

169 which 49% are C–I type branches, 29% are C–C branches and 22% are I–I branches marking completely separated

170 lineaments. Topological parameters are shown in Tab. 3.

171

172 **Tab. 3. Topological parameters of the network in analyse sectors**

	Western Silesian with Foremagura	Central Silesian	Eastern Silesian and Skole	Western Magura	Central Magura	Eastern Magura and Dukla	Whole area
	WS	**CS**	**ES**	**WM**	**CM**	**EM**	
No. of nodes (I+X+Y)	19	68	101	47	67	40	383
I nodes	8	51	76	26	48	36	293
X nodes	1	6	6	3	6	2	19
Y nodes	10	11	21	18	15	2	71
E nodes	22	38	49	46	61	52	-

C-C connections	11.5	14.5	18.5	21.0	33.5	3.0	77.0
C-I connections	8.5	28.5	35.5	22.0	25.0	11.5	131.0
I-I connections	1.0	11.0	23.5	3.0	14.0	10.5	81.0
No. of branches	21.0	54.0	77.5	46.0	54.5	25.0	291
No. of lines	9.0	31.0	48.5	22.0	31.5	19.0	182
No. of connections	11	17	25	21	19	4	90
Connects per line	2.44	1.10	1.03	1.91	1.21	0.42	0.99
Connects per branch	1.62	1.06	1.02	1.43	1.12	0.56	0.99
Dim.less intensity	1.21	0.87	1.21	1.65	1.33	2.06	0.75
Av. degree of network	2.21	1.59	1.53	1.96	1.63	1.25	1.52

173

174

175 The highest dimensionless intensity parameter is in the Eastern Magura and Dukla sector (2.05) and the lowest in

176 the Central Silesian (0.87). On the other hand, the Eastern Magura sector is characterised by the lowest connections

177 per branch (0.56) or the average degree of network (1.25) due to its form of mainly parallel features, with only

178 12% of the branches of connecting type (C–C). The best interconnectivity is observed in the Western Silesian

179 sector with 1.62 connections per branch and an average degree of the network of 2.21. This is an effect of the

180 presence of the Żywiec Basin block-system in the central part of the region.

181 The difference between these two (Eastern Magura and Western Silesia) sectors can be clearly visible on the

182 ternary diagrams (Fig. 4) presenting the relationships of the nodes and branch types. In the Western Silesian sector,

183 there is a high ratio of Y type nodes (52% of non-E-type nodes) and only one I–I branch.
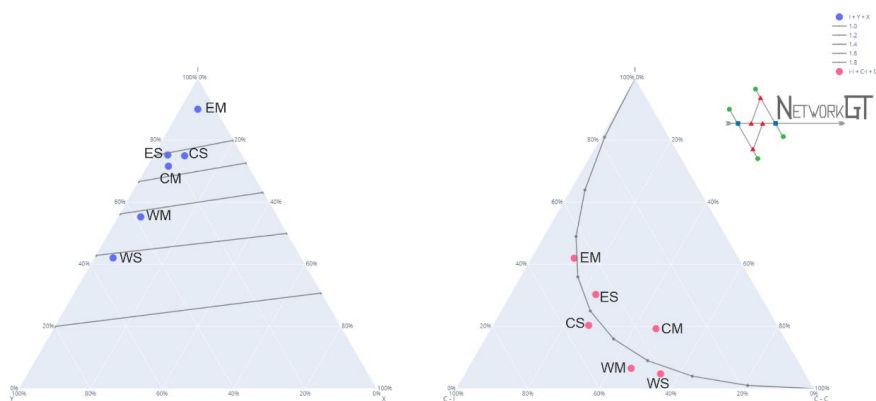
184

185 **Fig. 4: Ternary diagram presenting nodes (left) and branches (right) proportions in the analyse sectors.**

186

187 The parameters of all the other sectors fall between the Eastern Magura and Western Silesia sectors. The Western

188 Magura sector has quite good interconnectivity with a similar type of Eastern Magura blocky network.

189 Another approach to analysing topology is to use a sampling regular grid. The results are shown in Fig. 4 as maps

190 of connections per branch number, 2D network intensity and dimensionless intensity.

191 It can be seen that in terms of connections per branch we have two relatively large regions with a high number.

192 The first one is in the Western Silesian and partially Western Magura sectors, that is, the Żywiec Basin area, but

193 from the geological point of view it is also a narrow zone of Foremagura units occurring between the Silesian and

194 Magura nappes. Moreover, the Subsilesian unit tectonic window occurs in this area.

195 The Nowy Sącz Basin (eastern part of the Central Magura sector in the subdivision used here) is the next region

196 with a high number of connections per network branch. The lineament system in this area surrounds a zone of

197 Neogene deposits lying on the Carpathian flysch and filling the intramountain Nowy Sącz Basin.

198 The 2D intensity map shows that the Nowy Sącz Basin is characterised in general by a higher intensity than the

199 Żywiec Basin. There is also a general trend of higher intensity in the western part of the Carpathians (especially

200 the Western Magura and Central Magura sectors) than in the eastern part (Eastern Magura and Dukla).

201 In terms of dimensionless intensity parameter there are two regions with significantly high values: the south-

202 eastern part of the Wiśnicz foothill, which is in the Central Silesian sector, and the eastern parts of the Beskid

203 Niski Mts. and Bukowiec foothill in the Eastern Magura and Eastern Silesian sectors, on the geographical border

204 of the Western and Eastern Carpathians.

205 **6.   Discussion**

206 **6.1   Different lineament identification approaches**

207 There are 110 photolineaments marked on the photogeological map of Poland in the studied area (Bażyński et

208 al., 1986). In the same area of the geological map of the Carpathians, Lexa et al. (2000) marked 2 325 features

209 described as a fault or assumed fault. In many cases, our lineament system seems to be concordant or

210 complimentary to Lexa et al.'s (Fig. 5). In some cases, the features marked as faults are rather thrust lines, as per

211 the Fig. 5a example. The photolineament system is in general concordant with the DEM-interpreted system.

212 Visual inspection of the compiled lineaments map (Fig. 6a) shows that the especially NE striking lineaments of

213 the Eastern Magura sector are consistent with each other. Moreover, the system framing the Żywiec tectonic

214 window is well visible in both sets. On the other hand, there are some photolineaments that are not recognisable

215 on the DEM, and in fact also hardly visible on the modern orthophoto map. The most prominent example are two

216 straight, parallel lineaments striking the NNE in the central part of the study area, cutting its entire width. These

217 features seem to cut Gorce Mts.; this is not confirmed by our other studies (Kania and Szczęch, 2020; Szczęch

218 and Cieszkowski, 2021). Further to the north, these two lineaments are delimiting massifs of the Beskid

219 Wyspowy Mts. (Mogielica, Łopień). These massifs are in fact particularly visible on the aerial photo, as rather

220 isometric 'islands', and are formed by core parts of the synclines (Wójcik et al., 2009). On the other hand, some

221 lineament systems well visible in DEM are not marked on the photolineament map, as per the case of the system

222 north of the Nowy Sącz. That shows how these two methods can in fact be recognised as complementary

223 approaches to the lineaments' identification.

224 The system from the map by Lexa et al. (2000) shows confirmed and inferred faults, which is why it is not fully

225 compatible with lineaments; the lineaments, even when mainly tectonic related, are in fact a broader term (O'Leary

226 et al., 1976). Especially, these data, despite being a very rich collection of features are not applicable for topological

227 analyses: most of the features are short and isolated even when forming a network. Nevertheless, these data include

228 faults that are identified with geological criteria that are not visible in the remote sensing (at least at the scale

229 applied in this paper or by Bażyński et al., 1986 photolineament map. These data are augmenting each other, which

230 is highly visible in the Piwniczna Zdrój area, where DEM interpreted that the NNW striking lineament along the

231 Poprad River Valley (not present in the photolineament set) is flanked with a set of N or NNE striking faults,

232 which we have not identified on the DEM.

233
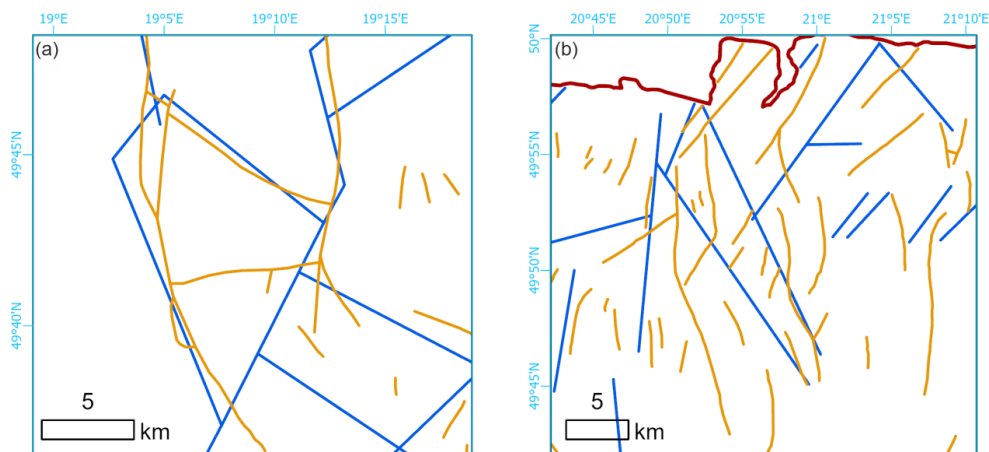
234 **Fig. 5. Comparison of lineament system detected from the GMETD model (blue) and faults by Lexa et al.,**

235 **2000 (brown). (a) Żywiec Basin area, (b) fragment of the Zakliczyn – Olszyny fault zone.**
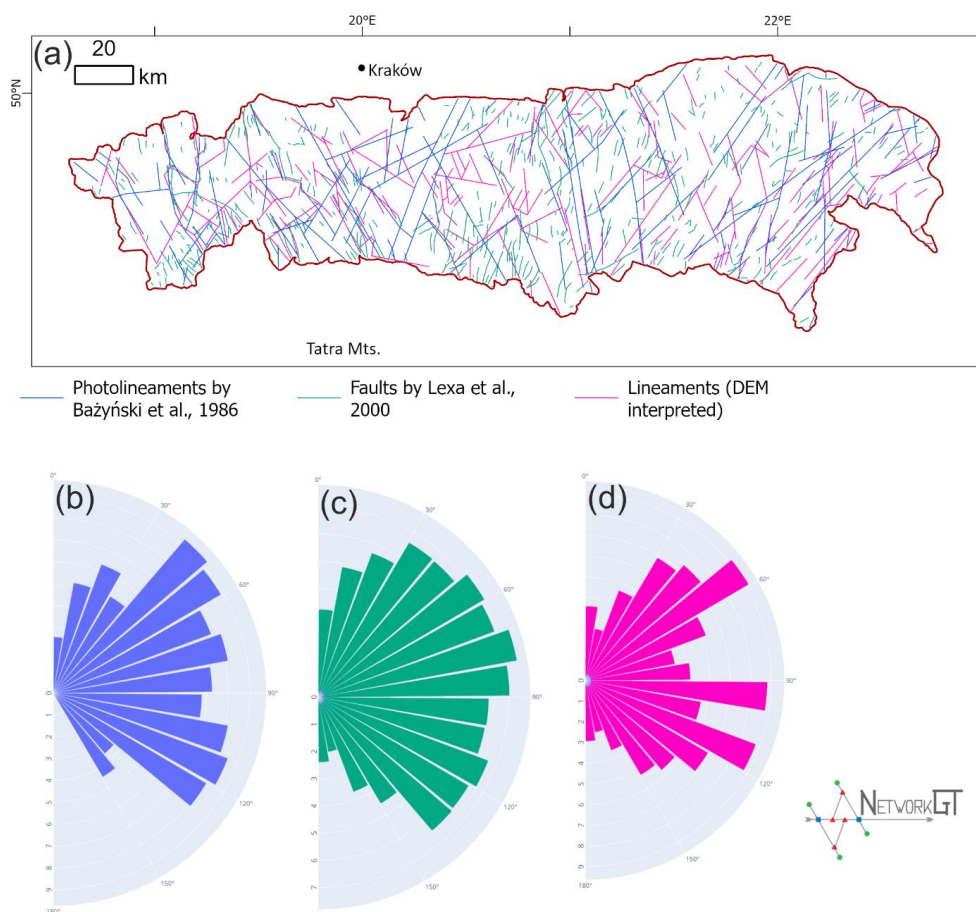
Fig. 6. Geometry of lineament networks in the Carpathians. (a) compilation map of lineaments by Bażyński et al., 1986, faults by Lexa et al., 2000 and lineaments interpreted from DEM in the presented paper. (b-d) rosediagrams of features azimuth in the whole study area from: (b) Bażyński et al. (1986), (c) Lexa et al., 2000 and (d) DEM interpreted.

When analysing the distribution of feature azimuth for the whole study area (Fig. 6b-d), it can be noted that the directions for the photolineament set (B) and DEM-interpreted set (D) are quite similar. What is noteworthy is the lack of azimuths greater than 150° in the photo set, which are present (albeit in a minority) in the DEM set. Furthermore, the photo set shows two maxima, at ca. 45° and 110°, whilst in the DEM set there are three maxima at ca. 50°, 100° and 110°. However, the dominating directions are not in fact distributed uniformly along the W–E span of the Polish Western Carpathians, which can be clearly seen in Fig. 6a where the domination of NE directions in the eastern sectors can be noticed, as well as the presence of two main directions in the western and central sectors.

6.2 Dominating directions of the lineament network

250

251 We observed a difference in dominating azimuths of lineaments between the western/central sectors (WS, WM,

252 CS, CM) and eastern sectors (ES, EM) of the study area. The first ones are characterised by two distinct sets of

253 lineaments (NNE or NE and SE), while the second has an SE set that is strongly reduced.

254 According to the general tectonic model of the Outer Carpathians (Unrug, 1980), the flysch deposits are cut by

255 set sinistral strike–slip fault zones. These fault zones are arranged in a fan-like shape along the arc of the

256 Carpathians, leading to the rotation of the set of nappes (Unrug, 1980; Graniczny and Mizerski, 2003). The

257 observed trend of increasing importance of the NE direction to the east is consistent with this model. However,

258 the more complicated geometry of the western part of the network may be related to the more complicated

259 system of the deep-rooted fault zones in this part (see further discussion below).

6.3 Topological differentiation of the network

260

261 There are no topological analyses of the lineament networks for the Outer Carpathians. Our previous article

262 (Kania and Szczęch, 2022) was focused on one mountain massif: Gorce Mts. From the tectonic point of view,

263 this massif is quite homogenous, being located in the one tectono-facial unit (Magura unit) with some subunits

264 within (Bystrica and Krynica subunits). Therefore, the paper focused mainly on different litostratigraphic units,

265 showing how different types of lithology differ in topology terms.

266 Scaling the research into the Polish Western Carpathians shows that in general there are no differences in the

267 network topology related to the tectono-facial units (Outer Carpathian nappes) since in general, all these units are

268 similar in lithology (flysh packets). However, there are differences related to some irregularities in tectonics:

269 especially, the intramountain basins are marked with increased network interconnectivity. The western part of the

270 study area in general has a better developed network. Especially, the Eastern Magura differs from the rest of the

271 sectors: the domination of one lineament direction results in low network interconnectivity, which is expressed by

272 a high proportion of the I nodes and I–I branches (Fig. 4). We analysed Magura unit and part of the Dukla unit

273 together; however, the interconnectivity in the Dukla Nappe (belonging to the Foremagura group) is stronger than

274 in Magura, which can be related to the proximity of the Silesian unit overthrust.

275 The highest interconnectivity was observed in the Western Silesian sector. The area is characterised by a high

276 proportion of Y nodes, and thus mainly by the presence of C–I or C–C branches (Fig. 4). In the geological

277 context, it is related to the location of the Żywiec tectonic window, which exposes the Subsilesian unit.

278 However, the topological study shows that the tectonised zone is wider; the increase in connections per branch

279 zone continues to the south along the Soła River and further, at least to the state border in the Beskid Żywiecki

280 Mts.

6.4 Main large-scale, deep-rooted lineament systems of the Western Carpathians and their relation to DEM-interpreted lineaments

281

282

283 The following, well-known, large-scale lineaments reach the Carpathian basement cutting the Polish part of the

284 Outer Western Carpathians (Doktór et al., 1985): Central Slovakia, Myjava, Muran, Štitnik and Przemyśl. There

285 are also lineaments not named by Doktór et al. (1985), but striking parallel, approximately 10 km to the east from

286 the Skawa fault zone (Cieszkowski et al., 2006). Fig. 7 presents the generalised positions of the lineaments.
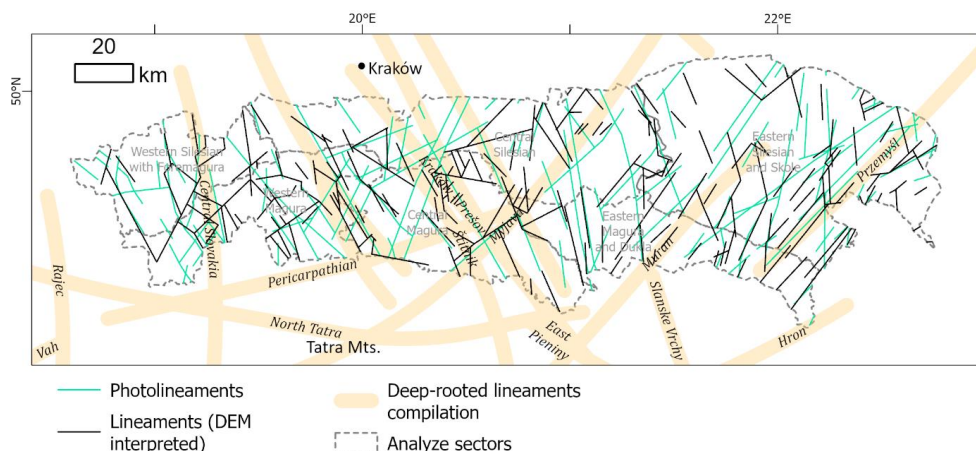
Fig. 7. Interpreted lineament system with photolineaments by Bażyński et al., 1986 as well as deep-rooted
lineament compilation after Sikora, 1976; Zuchiewicz, 1984; Doktór et al., 1985.

The central Slovak line marks the eastern border of the Żywiec basin and marks the major fault zone well visible
in the displacing Fore–Magura belt near Żywiec. Some of the lineaments belonging to the system can also be
traced to the east, with some connecting NE–SW branches near the northern margin of the Carpathians.

The system of Muran lineaments in the discussed region is marked by a few short NE–SW lineaments in the eastern
sectors of the Magura and Silesian units. The Myjava system, in fact one of the most prominent systems in the
Carpathians, in the study area can be traced along the Nowy Sącz Basin, continuing to the north where there is a
series of short lines parallel to the zone lineaments. The network interconnectivity increases in this area. The
lineaments there lie in an extension of the Carpathian Shear Corridor, a large-scale strike–slip zone between Vienna
and the High Tatra Mts. (Marko et al., 2017). Although the Štitnik system is unclear, some parallel or subparallel
lineaments can be assigned to this zone. The Przemyśl lineament zone is identified as a set of long lineaments in
the easternmost parts of the area, where the main features of NE–SW are possibly interconnected by shorter N–S
lines, forming an interconnected, blocky, two-set system.

Another important deep-rooted linear structure, confirmed by a negative gravimetric anomaly is the Pericarpathian
line, which runs along the Nowy Sącz–Nowy Targ–Kysucké Nové Mesto line (Zuchiewicz, 1984; Sikora, 1976),
which runs similarly to the Myjava structure. The Kraków–Prešov lineament, which is an extension of the
Kraków–Lubliniec fault zone and marks the border between the Małopolska and Brunovistulicum blocks of the
basement (Żaba, 1999; Zuchiewicz, 1984), runs along the Dunajec Valley. A system of lineaments is clearly visible
along this line, mainly in the Magura Nappe; however, parallel photolineaments were marked even longer to the
north (Bażyński et al., 1986).

These systems can be arranged in two sets: NNW, NW–SSE, SE striking (Central Slovakia, Skawa, Kraków–
Presov and Štitnik); and NE–SE (Myjava and Pericarpathian, Muran and Przemyśl). That implies some points of
system intersection, and in the area analysed such a place is in the Nowy Sącz region. This place is characterised
by higher interconnection factors (Fig. 8), in relation to the surrounding area. Moreover, in terms of

315 geomorphology, this is an intramountainous basin, being the only location where deposits are observed in the

316 Magura Nappe Neogene.

0   25   50 km

317

318
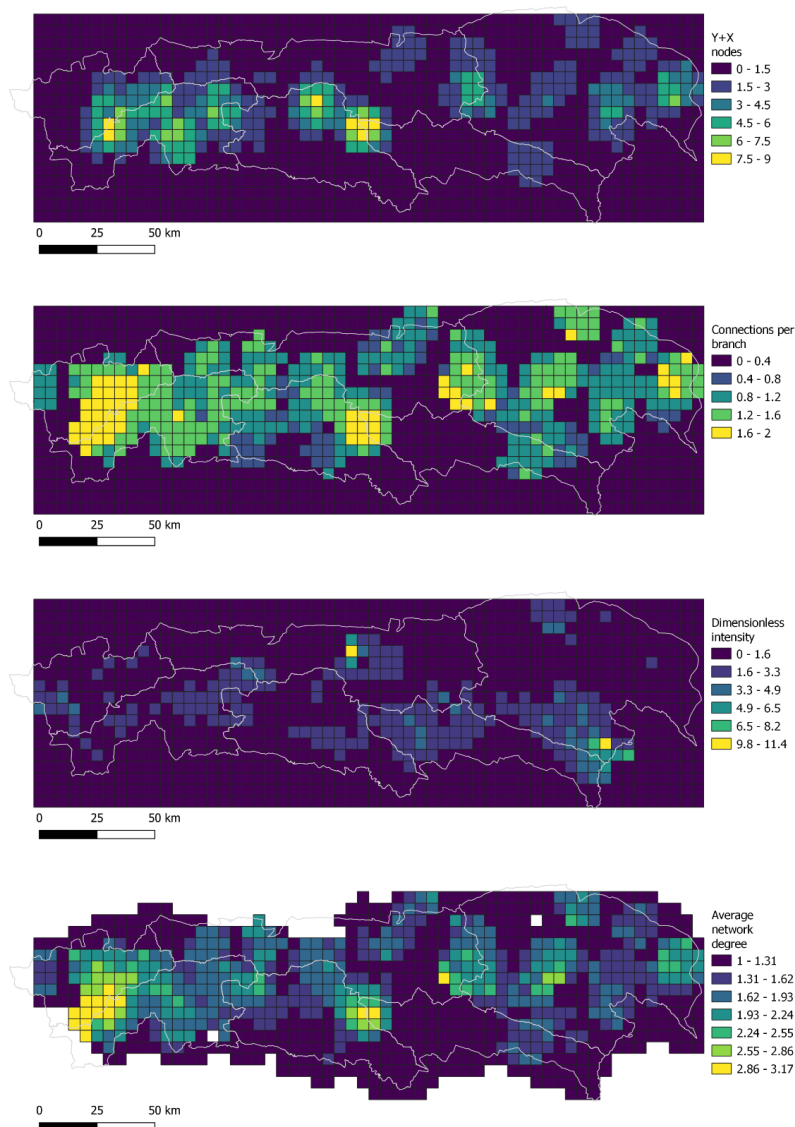
Fig. 8. Topological parameters of the lineament network, from up to down: connections per branch number,

dimensionless intensity factor, and average network degree.

321

322 The Central Slovakian system strikes along the east border of the Żywiec Basin and Żywiec tectonic window,

323 where the Subsilesian Nappe is exposed. We also marked a major lineament there, which is not present on the

324 photolineament map (Bażyński et al., 1986) or the database of the Western Carpathian Geological Map (Lexa et

325 al., 2000). The lineament (in the central part, the Soła River Valley) cuts the Magura Nappe, the Foremagura zone

326 with Magura overthrust and the Silesian Nappe. This structure is one of the edges of the rhomboidal block, in

327 which the Żywiec Basin has been developed. The generally increased degree of network interconnection (Fig. 8)

328 and the intensity of the network in this area can be an effect of the interaction between the central Slovakian system

329 with the Soła lineament and all the lowered block edges.

330 The cross-cutting relations of the Myjava lineament and the Stitnik lineament, whose continuation can be the

331 Dunajec fault system, are reflected in the bimodality of lineaments. The dominating maximum in the central

332 Magura sector, at approximately 120°, is similar to the Stitnik lineament; however, the Myjava lineament is

333 reflected there by just a few dominating lineaments, which are relatively long. Moreover, the Pericarpathian

334 lineaments are also known in this region. This structure, reflected in the sedimentary cover as the Dunajec fault

335 zone, is also confirmed by a negative gravimetric anomaly (Zuchiewicz, 1984; Sikora, 1976). Another deep

336 structure cutting this area is the Kraków–Presov fault, which is an extension of the Kraków–Lubliniec fault zone

337 under the Carpathians active to the Quternary (Żaba, 1999). All these deep cross-cutting features result in an

338 increased degree of the network connectivity observed on the surface. Then, the blocky structure allowed the

339 formation of an intramountain basin, filled with Neogene sediments.

340

341 Topological analysis also suggests that the well-known Skawa fault zone (Zuchiewicz et al., 2009; Unrug, 1980)

342 is in fact the western-most part of the wider zone of increased network interconnectivity, extending ca. 10–20 km

343 to the west of the Raba River.

344 **7. Conclusions**

345 The proposed data source and analysis method are complementary with other lineament analysis from the study

346 area. The observed azimuths are in general concordant with the photolineament network; however, there are some

347 structures that are not confirmed by DEM interpretation. The relationship between the DEM-interpreted data and

348 geologically confirmed faults shows the usefulness of DEM as a data source in fault detection.

349 The dominating directions of the network are typical for the Western Carpathians, with a clear increase of the NE

350 striking features proportion towards the east.

351 The topological properties of the lineament network in the Western Carpathians show E–W trends, but no clear

352 S–N (perpendicular to the tectonic units) trends. This justifies the proposed subdivision of the Carpathians in the

353 western, central and eastern sectors in addition to the tectono-facial subdivision. The eastern sectors are dominated

354 by NE–SW trends and low interconnectivity, while the central and western sectors are more interconnected and

355 characterised by cross-cutting relationships of two main lineament directions. The degree of network

356 interconnectivity increases in areas with a lower morphology (intramountainous basins): the Żywiec Basin and

357 Nowy Sącz Basin.

358 The geometry of the network, in general, reflects a system of deep-rooted lineaments. The cross-cutting area of

359 the main deep lineaments is reflected in stronger network interconnectivity in the Nowy Sącz area.

360

361 CRediT authorship contribution statement: Maciej Kania: Conceptualization, Methodology, Formal analysis,

362 Investigation, Writing - original draft, Visualization. Mateusz Szczęch: Investigation, Writing - review &

363 editing, Visualization.

364

365 Declaration of competing interest: The authors declare that they have no known competing financial interests or
366 personal relationships that could have appeared to influence the work reported in this paper

367
368 Acknowledgements: The research was financed from funds of the Jagiellonian University Institute of
369 Geological Sciences. Proofreading of this publication has been supported by a grant from the Priority
370 Research Area (Digiworld) under the Strategic Programme Excellence Initiative at Jagiellonian University.

371 **References**

372 Baas, J. H.: EZ-ROSE: a computer program for equal-area circular histograms and statistical analysis of two-
373 dimensional vectorial data, Comput Geosci, 26, 153–166, https://doi.org/10.1016/S0098-3004(99)00072-2,
374 2000.

375 Bażyński, J., Doktór, S., and Graniczny, M.: Mapa fotogeologiczna Polski w skali 1:1 000 000, 1986.

376 Chodyń, R.: Zastosowanie cyfrowego modelu terenu (DEM) w badaniach geologicznych na przykładzie obszaru
377 między Dobczycami a Mszaną Dolną (polskie Karpaty zewnętrzne), Przeglad Geologiczny, 52, 315–320, 2004.

378 Cieszkowski, M., Golonka, J., Waśkowska-Oliwa, A., and Chrustek, M.: Budowa geologiczna rejonu Sucha
379 Beskidzka - Świnna Poręba (polskie Karpaty fliszowe), Geologia / Akademia Górniczo-Hutnicza im. Stanisława
380 Staszica w Krakowie, 32, 155–201, 2006.

381 Cieszkowski, M., Kysiak, T., Szczęch, M., and Wolska, A.: Geology of the Magura Nappe in the Osielec area
382 with emphasis on an Eocene olistostrome with metabasite olistoliths (Outer Carpathians, Poland), Annales
383 Societatis Geologorum Poloniae, 87, 169–182, https://doi.org/10.14241/asgp.2017.009, 2017.

384 Danielson, J. J.: Global Multi-resolution Terrain Elevation Data 2010 (GMTED2010) Coastal Elevation
385 Modeling View project LP DAAC View project, 2011.

386 Doktór, S. and Graniczny, M.: Geologiczna interpretacja zdjęć satelitarnych i radarowych wschodniej części
387 Karpat, Kwartalnik Geologiczny, 26, 231–245, 1982.

388 Doktór, S. and Graniczny, M.: Fotogeologiczna analiza zdjęć satelitarnych Karpat, Kwartalnik Geologiczny, 27,
389 645–656, 1983.

390 Doktór, S., Dornic, J., Graniczny, M., and Reichwalder, P.: Structural elements of Western Carpathians and their
391 Foredeep on the basis of satellite interpretation, Geological Quarterly, 29, 129–138, 1985.

392 Doktór, S., Graniczny, M., Kucharski, R., Molek, M., and Dąbrowska, B.: Wgłębna budowa geologiczna Karpat
393 w świetle kompleksowej analizy teledetekcyjno-geofizycznej, Przegląd Geologiczny, 38, 469–475, 1990.

394 Doktór, S., Graniczny, M., Kowalski, Z., and Wójcik, A.: Możliwości zastosowania wyników interpretacji zdjeć
395 radarowych do analizy tektonicznej Karpat, Przeglad Geologiczny, 50, 852–860, 2002.

396 Ehlen, J.: Lineation, edited by: Goudie, A. S., Encyclopedia of Geomorphology, 2, 623–624, 2004.

397 Golonka, J., Aleksandrowski Pawełand Aubrecht, R., Chowaniec, J., Chrustek, M., Cieszkowski, M., Florek, R.,
398 Gawęda, A., Jarosiński, M., Kępińska, B., and others: The Orava deep drilling project and post-palaeogene
399 tectonics of the northern Carpathians, Annales Societatis Geologorum Poloniae, 75, 211–248, 2005.

400 Golonka, J., Waśkowska, A., and Ślączka, A.: The Western Outer Carpathians: Origin and evolution, Zeitschrift
401 der Deutschen Gesellschaft für Geowissenschaften, 229–254, 2019a.

402 Golonka, J., Waśkowska, A., and Ślączka, A.: The western outer carpathians: Origin and evolution, Zeitschrift

403 der Deutschen Gesellschaften fur Geowissenschaften, 170, 229–254, https://doi.org/10.1127/zdgg/2019/0193,

404 2019b.

405 Golonka, J., Gawęda, A., and Waśkowska, A.: Carpathians, Reference Module in Earth Systems and

406 Environmental Sciences, 1–10, https://doi.org/10.1016/b978-0-12-409548-9.12384-x, 2020.

407 Graniczny, M. and Mizerski, W.: Lineamenty na zdjęciach satelitarnych Polski - próba podsumowania, Przegląd

408 Geologiczny, 51, 474–482, 2003.

409 Kania, M. and Szczęch, M.: Geometry and topology of tectonolineaments in the Gorce Mts. (Outer Carpathians)

410 in Poland, J Struct Geol, 141, 104186, https://doi.org/10.1016/j.jsg.2020.104186, 2020.

411 Kania, M. and Szczęch, M.: Tectonic Structures Interpretation Using Airborne-Based LiDAR DEM on the

412 Examples from the Polish Outer Carpathians, in: Atlas of Structural Geological and Geomorphological

413 Interpretation of Remote Sensing Images, edited by: Misra, A. A. and Mukherjee, S., 157–165, 2022.

414 Książkiewicz, M.: The Tectonics of the Carpathians, in: Geology of Poland, vol. 4. Tectonics. The Alpine

415 Tectonic Epoch, Geological Institute, Warszawa, 476–608, 1977.

416 Leech, D. P., Treloar, P. J., Lucas, N. S., and Grocott, J.: Landsat TM analysis of fracture patterns: A case study

417 from the Coastal Cordillera of northern Chile, Int J Remote Sens, 24, 3709–3726,

418 https://doi.org/10.1080/0143116031000102520, 2003.

419 Lexa, J., Bezák, V., Elečko, M., Mello, J., Polák, M., and Vozár, J.: Geological map of western Carpathians and

420 adjacent areas 1:500 000, 2000.

421 Mahel', M.: Tectonics of the Carpathian–Balkan Regions, Explanations to the Tectonic Map of the Carpathian-

422 Balkan Regions and Their Foreland., Štátny geologický ústav Dionýza Štúra, Bratislava, 180–197 pp., 1974.

423 Marko, F., Andriessen, P. A. M., Tomek, Č., Bezák, V., Fojtíková, L., Bošanský, M., Piovarči, M., and

424 Reichwalder, P.: Carpathian Shear Corridor – A strike-slip boundary of an extruded crustal segment,

425 Tectonophysics, 703–704, 119–134, https://doi.org/10.1016/j.tecto.2017.02.010, 2017.

426 van der Meer, F. D., van der Werff, H. M. A., van Ruitenbeek, F. J. A., Hecker, C. A., Bakker, W. H., Noomen,

427 M. F., van der Meijde, M., Carranza, E. J. M., de Smeth, J. B., and Woldai, T.: Multi- and hyperspectral geologic

428 remote sensing: A review, https://doi.org/10.1016/j.jag.2011.08.002, 2012.

429 Minár, J., Bielik, M., Kováč, M., Plašienka, D., Barka, I., Stankoviansky, M., and Zeyen, H.: New

430 morphostructural subdivision of the Western Carpathians: An approach integrating geodynamics into targeted

431 morphometric analysis, Tectonophysics, 502, 158–174, 2011.

432 Motyl-Rakowska, J. and Ślączka, A.: Ważniejsze lineamenty karpat i ich związek ze znanymi, Przegląd

433 Geologiczny, 32, 72–77, 1984.

434 Mukherjee, S.: Using Graph Theory to Represent Brittle Plane Networks, 259–271,

435 https://doi.org/10.1016/B978-0-12-814048-2.00022-3, 2019.

436 Introducing Esri's Next Generation Hillshade: https://www.esri.com/arcgis-blog/products/arcgis-living-

437 atlas/imagery/introducing-esris-next-generation-

438   hillshade/?rmedium=redirect&rsource=blogs.esri.com/esri/arcgis/2014/07/14/introducing-esris-next-generation-

439   hillshade, last access: 1 June 2022.

440   Nyberg, B., Nixon, C. W., and Sanderson, D. J.: NetworkGT: A GIS tool for geometric and topological analysis

441   of two-dimensional fracture networks, Geosphere, 14, 1618–1634, https://doi.org/10.1130/GES01595.1, 2018.

442   O'Leary, D. W., Friedman, J. D., and Pohn, H. A.: Lineament, linear, lineation: Some proposed new standards

443   for old terms, Geological Society of America Bulletin1, 87, 1463–1469, 1976.

444   Oszczypko, N.: Late Jurassic-Miocene evolution of the Outer Carpathian fold-and-thrust belt and its foredeep

445   basin (Western Carpathians, Poland), Geological Quarterly, 50, 169–194, 2006.

446   Ozimkowski, W.: Lineamenty otoczenia Tatr - porównanie interpretacji DEM i MSS, Przegląd Geologiczny, 56,

447   1099–1102, 2008.

448   Plašienka, D.: Continuity and episodicity in the early Alpine tectonic evolution of the Western Carpathians: How

449   large-scale processes are expressed by the orogenic architecture and rock record data, Tectonics, 37, 2029–2079,

450   2018.

451   Procter, A. and Sanderson, D. J.: Spatial and layer-controlled variability in fracture networks, J Struct Geol, 108,

452   52–65, https://doi.org/10.1016/j.jsg.2017.07.008, 2018.

453   Sanderson, D. J. and Nixon, C. W.: The use of topology in fracture network characterization, J Struct Geol, 72,

454   55–66, https://doi.org/10.1016/j.jsg.2015.01.005, 2015.

455   Sanderson, D. J., Peacock, D. C. P., Nixon, C. W., and Rotevatn, A.: Graph theory and the analysis of fracture

456   networks, J Struct Geol, 14th April, https://doi.org/10.1016/j.jsg.2018.04.011, 2018.

457   Scheiber, T., Fredin, O., Viola, G., Jarna, A., Gasser, D., and Łapińska-Viola, R.: Manual extraction of bedrock

458   lineaments from high-resolution LiDAR data: methodological bias and human perception, 137, 362–372,

459   https://doi.org/10.1080/11035897.2015.1085434, 2015.

460   Sikora, W.: On lineaments found in the Carpathians, Annales Societatis Geologorum Poloniae, 46, 3–37, 1976.

461   Ślączka, A., Kruglov, S., Golonka, J., Oszczypko, N., and Popadyuk, I.: Geology and hydrocarbon resources of

462   the Outer Carpathians, Poland, Slovakia, and Ukraine: general geology, The Carpathians and their foreland:

463   Geology and hydrocarbon resources: AAPG Memoir, 84, 221–258, 2006.

464   Solon, J., Borzyszkowski, J., Małgorzata Bidłasik, Richling, A., Badora, K., Balon, J., Brzezińska-Wójcik, T.,

465   Chabudziński, Ł., Dobrowolski, R., Grzegorczyk, I., Jodłowski, M., Kistowski, M., Kot, R., Krąż, P., Lechnio,

466   J., Macias, A., Majchrowska, A., Malinowska, E., Migoń, P., Myga-Piątek, U., Nita, J., Papińska, E., Rodzik, J.,

467   Strzyż, M., Terpiłowski, S., Ziaja, W., and Paul, J.: Physico-geographical mesoregions of Poland: verification

468   and adjustment of boundaries on the basis of contemporary spatial data, Geographia Polonica, 91, 143–170,

469   https://doi.org/10.7163/GPol.0115, 2018.

470   Szczęch, M. and Cieszkowski, M.: Geology of the Magura Nappe, south-western Gorce Mountains (Outer

471   Carpathians, Poland), J Maps, 17, 453–464, https://doi.org/10.1080/17445647.2021.1950579, 2021.

472   Teisseyre, W.: O związku w budowie tektonicznej Karpat i ich przedmurza, Kosmos, 32, 393–402, 1907.

473   Statistics (scipy.stats) — SciPy v1.9.3 Manual: https://docs.scipy.org/doc/scipy/tutorial/stats.html, last access: 8

474   November 2022.

475   Thiele, S. T., Jessell, M. W., Lindsay, M., Ogarko, V., Wellmann, J. F., and Pakyuz-Charrier, E.: The topology

476   of geology 1: Topological analysis, J Struct Geol, 91, 27–38, https://doi.org/10.1016/J.JSG.2016.08.009, 2016.

477   Unrug, R.: Tectonic rotation of flysch nappes in the Polish Outer Carpathians, Rocznik Polskiego Towarzystwa

478   Geologicznego, 50, 27–39, 1980.

479   Valentini, L., Perugini, D., and Poli, G.: The "small-world" topology of rock fracture networks, Physica A:

480   Statistical Mechanics and its Applications, 377, 323–328, https://doi.org/10.1016/j.physa.2006.11.025, 2007.

481   Wójcik, A., Czerwiec, J., and Krawczyk, M.: Szczegółowa Mapa Geologiczna Polski 1:50 000. arkusz

482   Limanowa, 2009.

483   Yang, L., Meng, X., and Zhang, X.: SRTM DEM and its application advances,

484   https://doi.org/10.1080/01431161003786016, 2011.

485   Żaba, J.: Ewolucja strukturalna utworów dolnopaleozoicznych w strefie granicznej bloków górnośląskiego i

486   małopolskiego, Prace Państwowego Instytutu Geologicznego, 166, 1–162, 1999.

487   Zuchiewicz, W.: The late Neogene - Quaternary tectonic mobility of the Polish West Carpathians - a case study

488   of the Dunajec drainage basin, Annales Societatis Geologorum Poloniae, 54, 133–189, 1984.

489   Zuchiewicz, W., Tokarski, A. K., Świerczewska, A., and Cuong, N. Q.: Neotectonic Activity of the Skawa River

490   Fault Zone (Outer Carpathians, Poland), Annales Societatis Geologorum Poloniae, 79, 67–93, 2009.

491

492

493